



5-2012

# Computer Simulation of Radiation Detection in Diamond Detectors

Travis Tune  
ttune@utk.edu

Follow this and additional works at: [http://trace.tennessee.edu/utk\\_chanhonoproj](http://trace.tennessee.edu/utk_chanhonoproj)

 Part of the [Physics Commons](#)

---

## Recommended Citation

Tune, Travis, "Computer Simulation of Radiation Detection in Diamond Detectors" (2012). *University of Tennessee Honors Thesis Projects*.  
[http://trace.tennessee.edu/utk\\_chanhonoproj/1563](http://trace.tennessee.edu/utk_chanhonoproj/1563)

This Dissertation/Thesis is brought to you for free and open access by the University of Tennessee Honors Program at Trace: Tennessee Research and Creative Exchange. It has been accepted for inclusion in University of Tennessee Honors Thesis Projects by an authorized administrator of Trace: Tennessee Research and Creative Exchange. For more information, please contact [trace@utk.edu](mailto:trace@utk.edu).

# **Computer Simulation of Radiation Detection in Diamond Detectors**

Travis Carver Tune

Department of Physics

Chancellor's Honors Program Senior Thesis

May 2012

The University of Tennessee, Knoxville

Faculty Advisor: Dr. Stefan Spanier

## Introduction

At accelerators around the world, such as the Large Hadron Collider (LHC) in Geneva, Switzerland, experiments are underway which address fundamental questions about the nature of the universe. At the Compact Muon Solenoid (CMS), for example, research is being done in order to find the elusive Higg's Boson, Matter-Anti-Matter asymmetries, and new particles not included in the Standard Model. Experiments at the LHC measure particles from proton collisions that occur at high speeds and luminosities. These secondaries create showers of particles in detector material whose energy can be measured. Solid state particle detectors are a crucial component in detecting and tracking charged particles.

At the innermost layer of the CMS detector is the Silicon Pixel Detector. Its inner most radius is only 5cm and therefore close to the proton beam. Because of the high luminosity and the confined space close to the beam track, radiation and heat present problems for particle detectors. Because of continued radiation damage, the silicon detector will have a reduced signal to noise ratio over time. For this reason, it is necessary to have a radiation hard detector material. Diamond is currently being researched as a prime substitute for future use in pixel detectors in high radiation environments. **(A. Oh., 1)**

To study the mechanism of radiation detection in diamond, we used a program called GEometry And Tracking (GEANT) which has been developed by the European Organization for Nuclear Research (CERN) for the computer simulation of the passage of particles through matter. **(Allison)** We first simulated a 100 GeV  $\pi^-$  as it interacted with diamond of dimension 4mm by 4mm by 500  $\mu\text{m}$ . We also simulated the effect of charge deposit close to the surface of the diamond by exposing it to a 5.5 MeV  $\alpha$  particle.

## Properties of Diamond

Diamond has a number of properties which make it viable for radiation detection. Diamond has a very large electron and hole mobility, which help to give it a very large thermal conductivity. This means that cooling the detector in places like the CMS becomes less difficult. It is also radiation hard, so its signal output over time in high radiation environments will not decrease as quickly as for silicon. **(Galbiati, 9)**

The diamond used for these detectors is made by the process of Chemical Vapor Deposition (CVD). In this process, a hydrocarbon gas is energized which causes carbon to build up in layers on pre-existing diamond powder. CVD diamond is built up layer by layer and can be monocrystalline or polycrystalline. **(Galbiati, 24)**

One important property of diamond is the trapping and detrapping of charge carriers due to grain boundaries or radiation damage. Grain boundaries occur in polycrystalline diamond and can be distributed randomly throughout the diamond. Monocrystalline diamond will be largely free of these grain boundaries. **(Millazo, 32)** In our simulations we considered an idealized single crystal diamond free of grain boundaries. Our simulated detector was 4mm by 4mm by 500  $\mu\text{m}$ .

## Detection Mechanism

The average energy loss  $\frac{dE}{dx}$  of a fast charge carrier through matter is given by the Bethe-Bloch Formula. **(Nakamura, 5)** For diamond, the energy loss is about  $6 \frac{\text{MeV}}{\text{cm}}$  **(Particle Data Group)**. For our 100 GeV  $\pi^-$  in our 500  $\mu\text{m}$  thick detector, we can expect on average an energy deposit of 300 keV in the diamond. The distribution of the energy loss is expected to be

according to a Landau function. This energy is lost through ionization, creating pairs of electrons and ions (holes) as it passes through the material. By applying a bias voltage across the detector, we generate an electric field which causes these secondary particles to drift. Moving secondary charged particles induce a current in the electrodes attached on either side of the diamond. **(Milazzo, 21)** By integrating the current via an external circuit using the Shockley-Ramo Theorem, one can obtain the charge induced on the electrodes. Figure 1 shows a sketch of the setup.

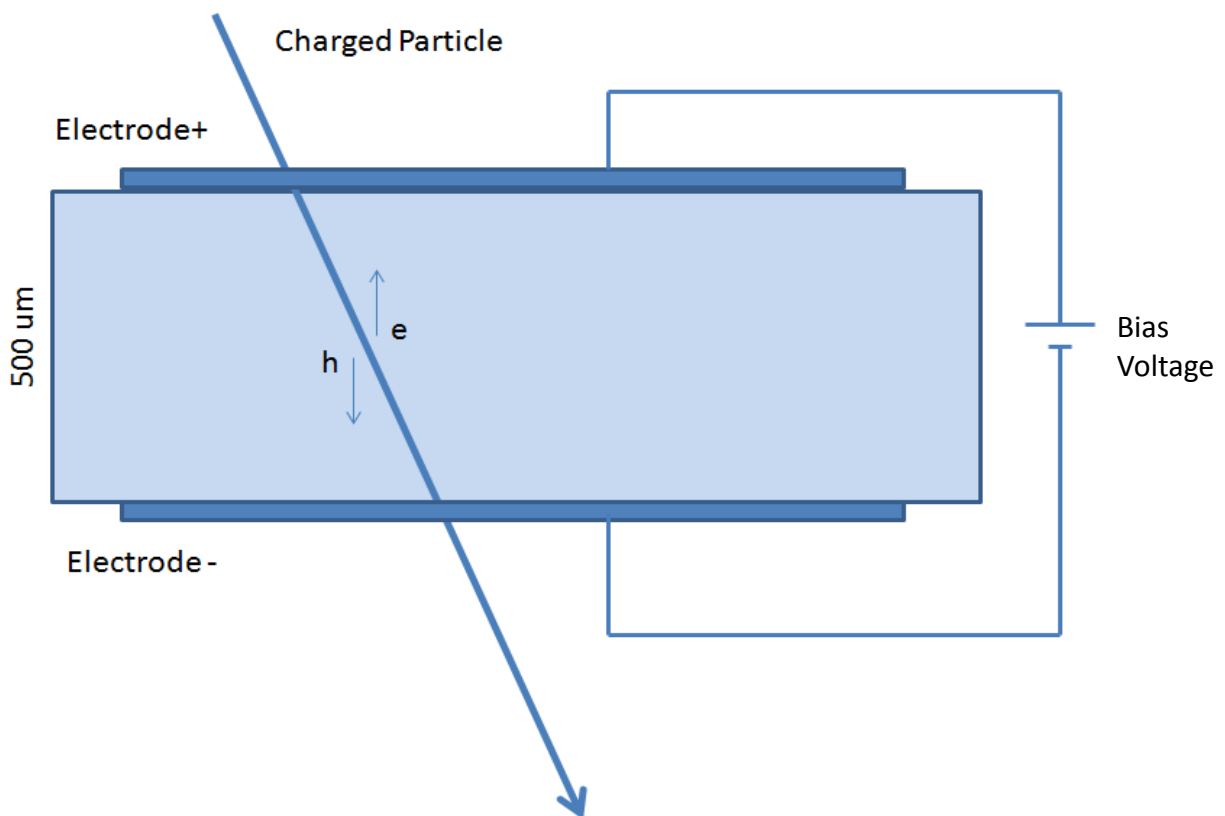


Figure 1: Detection Mechanism- drifting charges induce a current.

The charge carriers will also experience space charge effects, i.e. the buildup of charge carriers near the charge collecting electrode. Because the charged particles cannot leave the diamond instantaneously, it will lead to a broadened signal.

According to the Shockley-Ramo Theorem, the current induced by an electron moving near an electrode is related to the change in electrostatic flux lines, not the actual charge received by the electrode. The total induced charge  $Q$  is given as

$$Q = \int I dt = \int q \vec{v}(x, y) \cdot \vec{E}(x, y) \quad (1)$$

where  $\vec{v}$  is the velocity of secondary particles  $q$  is the charge of the particle, and  $\vec{E}$  is the normalized weighting field. The weighting field is given by  $\vec{E} = -\nabla \phi$  where  $\phi$  is the electric potential when the voltage on the readout electrode is set to unit potential and all other electrodes are grounded. **(Shockley)** Therefore we need to be able to simulate the electric field in our detector as well as know the properties of the charged secondary particles created by the initial ionizing particle. The program to simulate the electric field is called Poisson Superfish **(LAACG)**. It was applied for those secondary charged particles generated by GEANT. **(Allison)**

### **Electric Field**

The electric field causes the secondary charge carriers to drift towards the electrodes of the detector. Drifting charges induce a current which can be read in the external circuitry of the detector. Deep inside the detector, the field is approximately uniform. Near the boundaries and electrodes, however, it becomes highly dependent on the geometry of the detector. It is important to know the local electric field in the detector because the velocity of particles depends on it. At low fields the velocity of holes (h) and electrons (e),  $v_{e,h}$ , increases

linearly with the electric field as  $\vec{v}_{e,h} = \mu_{e,h}\vec{E}$ , where  $\mu_{e,h}$  is the mobility for electrons and holes.

At large fields  $\vec{v}_{e,h}$  will approach its saturated drift velocity. The typical field applied to diamond detectors is  $1\text{V}/\mu\text{m}$ . **(Pernegger, 1)** This field is large enough so that we can in good approximation assume that the secondary charge carriers travel at the saturated drift velocity.

For a more precise view of the electric field in our diamond detector, we used a program called Poisson Superfish. Poisson Superfish was developed by the Los Alamos Accelerator Code Group, and can be used to simulate 2D Electric or Magnetic Fields. The user can define boundaries and set the properties of the material. (LAACG) Figure 2 shows an example of an electric field map for a configuration of electrodes.

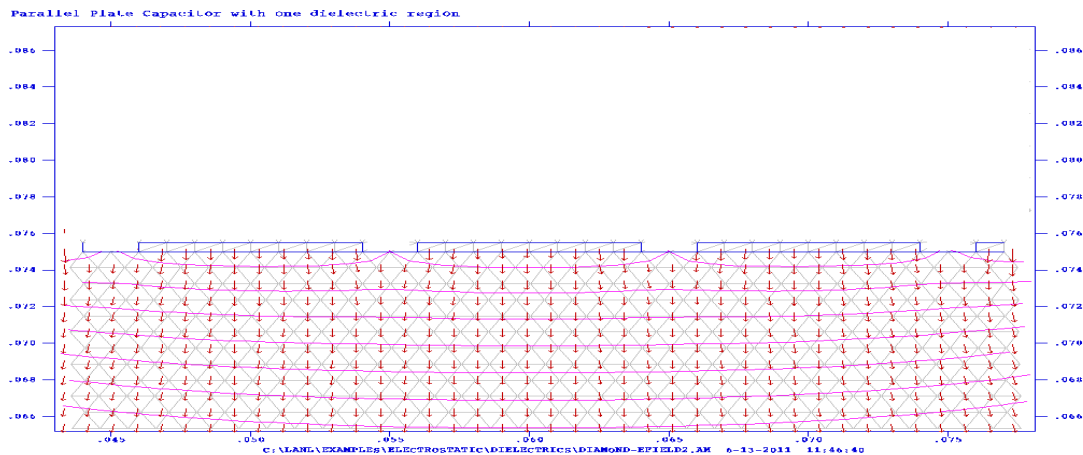


Figure 2: Electric Field Map near the electrodes.

## Simulating the Charge Carriers

In our GEANT simulations, we studied a 100 GeV  $\pi^-$  as well as a 5.5 MeV  $\alpha$  particle. At each step along the way, reactions are simulated according to a lookup table of cross sections when their likelihood is above a certain probability. Ionization is the main process involved and 13 eV is required to ionize an electron-hole pair in diamond. **(Milazzo, 53)**

A fast moving charge carrier in diamond will produce 36 electron-hole pairs per micrometer. From this we can estimate that on average 18,000 secondary charged particles will be created by the 100 GeV  $\pi^-$  in a 500 $\mu$ m thick layer of diamond. **(Milazzo, 52)** As for the  $\alpha$  particle, we know that the energy loss in diamond is  $6\frac{\text{MeV}}{\text{cm}}$ . Since it deposits its full 5.5 MeV in the diamond, we can expect that on average 400,000 secondary charged particles are produced.

## $\pi^-$ Simulation

First we examined the distribution around the average number of secondary particles created and the average amount of energy deposited by the 100 GeV  $\pi^-$ .

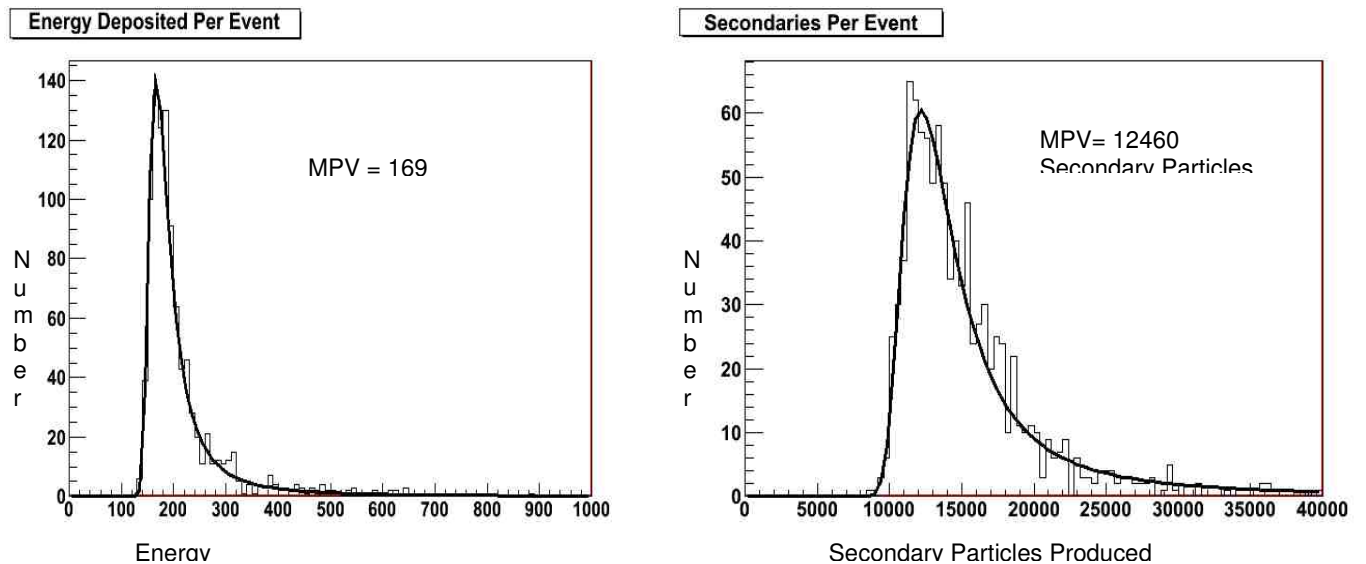


Figure 3: Left, distribution of energy deposited for 100 gev  $\pi^-$ ; Right, distribution of secondary particles produced



Figure 3, left, shows the distribution of energy deposited per event by a 100 GeV  $\pi^-$  for 1000 events, with the fit to a Landau curve superimposed. The most probable value (MPV) of these 1000 events was 169 keV. We can compare this to our mean estimate of 300 keV, which by definition is higher, from the Bethe-Bloch curve. Figure 3, right, shows the distribution in the number of secondary particles produced, also with the fit to a Landau curve superimposed. Our simulations predict a most probable value of 12000 secondary particles. We estimated a mean from Bethe-Bloch of 18000 using the energy deposit.

### **$\alpha$ Particle Simulation**

Because an  $\alpha$  particle stops in such a short distance in materials, depending on the sign of the bias voltage either the electrons or holes will be quickly captured at the electrode of the entrance surface, while the other will travel the full distance of the detector. This allows one to directly determine the current induced by the secondary charged particles produced by the  $\alpha$  particle traveling the full detector thickness.

The current measured is given as

$$I = \frac{qv}{d} \quad (2)$$

where we take  $v$  to be the saturated drift velocity,  $d$  is the width of the diamond, and  $q$  is the charge. Figure 4 shows the distribution of the measured current versus time for the  $\alpha$  particle.

## Current vs. Time

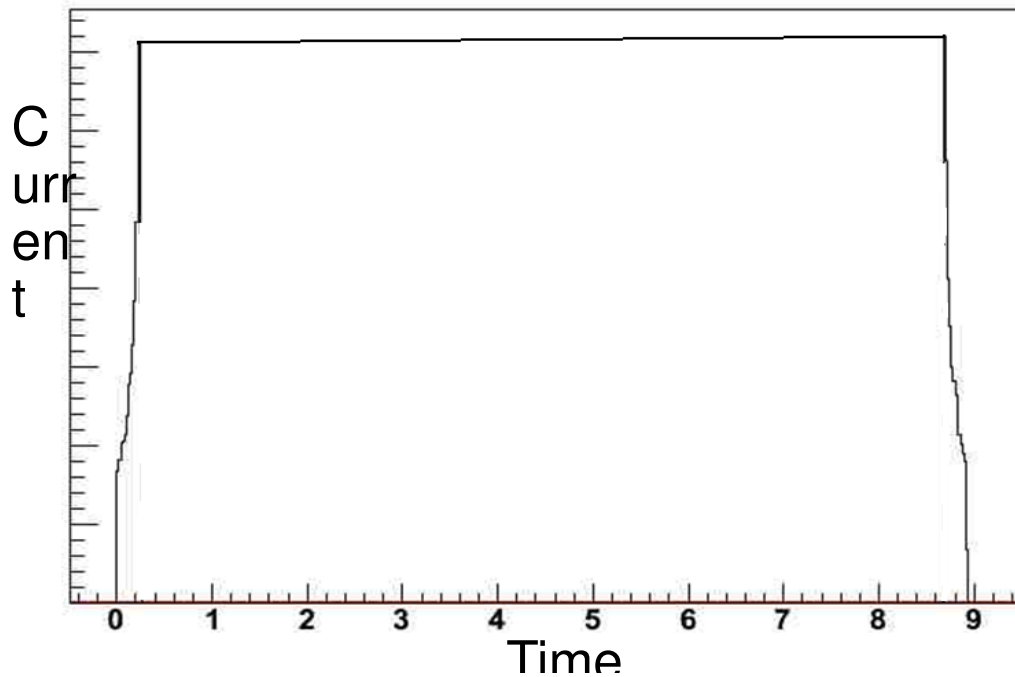


Figure 4: Measured Current Pulse Versus Charge Collection Time

Also, we can show the effect a global electric field has on our simulation. If we ignore edge effects we can assume a uniform field.

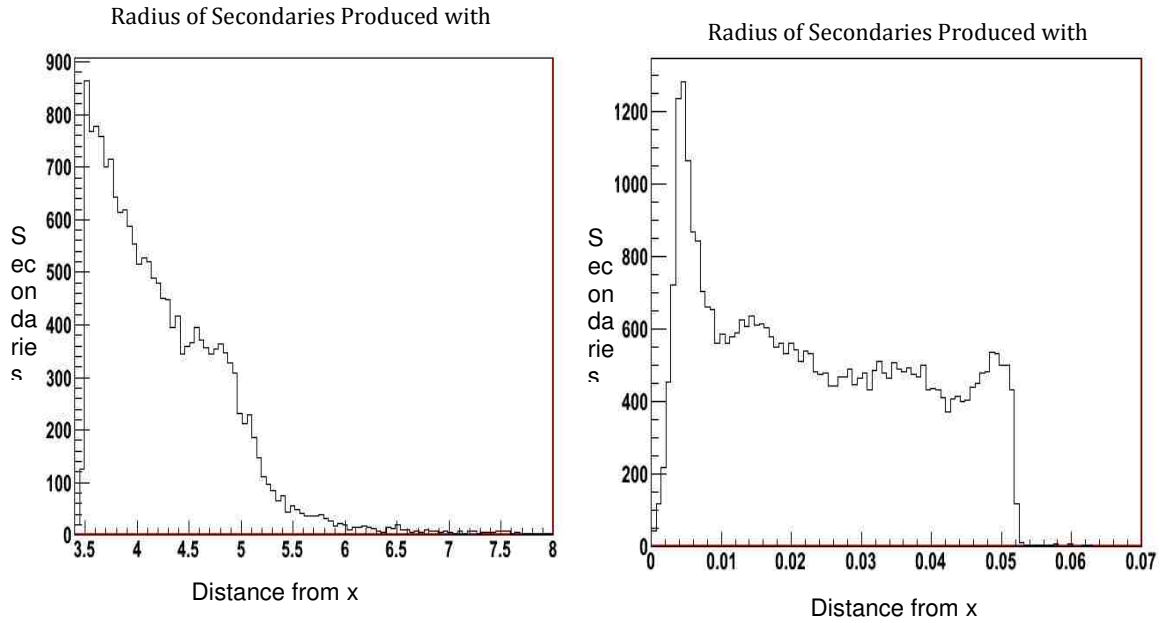


Figure 5: Global Electric Field

Figure 5 shows the distance of secondary charges from the primary particle track produced with and without an electric field. These plots demonstrate that the electric field pulls each secondary rapidly in its direction. This supports the assumption that secondary particles are instantaneously accelerated.

## Future Considerations

There are several effects which currently neglected in our diamond detector simulation. GEANT does not account for trapping and detrapping, space charge, or the local electric field in the diamond. To simulate these effects by ourselves, we will need to write a program which drifts the diamond through the detector in a 2D grid. In each step the program has to compute trapping and detrapping probabilities to determine whether the particle will be propagated. The effects of trapping and space charge for the induced current for electrons can be parameterized by the equation

$$i_{e,h}(t) \propto e^{\frac{t}{\tau_{effe,h}}} \cdot e^{\frac{-t}{\tau_{e,h}}} \quad (3)$$

where  $\tau_{effe,h}$  and  $\tau_{e,h}$  are time constants related to space charge and trapping, respectively.

**(Pernegger)**

## Works Cited

- Allison et al. "Geant4 developments and applications." IEEE Trans. Nucl. Sci. Volume 53. (2006).
- Galbiati, Arnaldo. *Development of CVD Diamond Radiation Detectors*. PhD Thesis, University of Surrey. (2003).
- Los Alamos Accelerator Code Group (LAACG). Poisson Superfish. (February 7, 2007). Los Alamos National Lab. Accessed June 2011  
<[http://laacg1.lanl.gov/laacg/services/download\\_sf.phtml](http://laacg1.lanl.gov/laacg/services/download_sf.phtml)>
- Milazzo, Lorenzo. *Computer Modelling of Diamond Radiation Detectors*. PhD Thesis, University of London. (2004)
- Nakamura *et al.* (Particle Data Group), J. Phys. G 37, 075021 (2010)
- Oh, A. *Particle Detection with CVD Diamond*. PhD Thesis, University of Hamburg. (1999).
- Particle Data Group. 2011. University of California. Accessed 2011  
<[http://pdg.lbl.gov/2011/AtomicNuclearProperties/HTML\\_PAGES/297.html](http://pdg.lbl.gov/2011/AtomicNuclearProperties/HTML_PAGES/297.html)>.
- Pernegger, et al. "Charge-carrier properties in synthetic single-crystal diamond measured with the transient-current technique." *Journal of Applied Physics* Volume 97. (2005).
- Shockley, W. "Currents to conductors Induced by a moving point charge." *Journal of Applied Physics* Volume 9. (1938).